GEOMETRIC AND TEMPORAL HEART CHARACTERIZATION USING DENSE HOUGH TRANSFORM IN CARDIAC MRI

Jean Alejandro Pico Velásquez

UNIVERSIDAD INDUSTRIAL DE SANTANDER
FACULTAD DE INGENIERÍAS FÍSICO-MECÁNICAS
ESCUELA DE INGENIERÍAS ELÉCTRICA, ELECTRÓNICA Y DE TELECOMUNICACIONES
BUCARAMANGA
2018

GEOMETRIC AND TEMPORAL HEART CHARACTERIZATION USING DENSE HOUGH TRANSFORM IN CARDIAC MRI

Jean Alejandro Pico Velásquez

A thesis presented in fulfillment of the requirements for the degree of Electronic Engineer

Advisor:
Fabio Martínez Carrillo
PhD in Systems and Computer Engineering

Co-Advisor:
Said David Pertuz Arroyo
PhD in Computer Science

UNIVERSIDAD INDUSTRIAL DE SANTANDER
FACULTAD DE INGENIERÍAS FÍSICO-MECÁNICAS
ESCUELA DE INGENIERÍAS ELÉCTRICA, ELECTRÓNICA Y DE TELECOMUNICACIONES
BUCARAMANGA
2018

Acknowledgements

This work would not have been possible without the efforts of my advisors Fabio Martínez and Said Pertuz. I would like to thank them for their patience and the many hours they spent providing insight, advice and direction.

Many thanks to my parents for being a source of stability and support in my life, allowing me to develop the present work in a comfortable way.

Many thanks to the School of Electric, Electronic and Telecommunications Engineering (E3T) and the Industrial University of Santander (UIS) for training me as a professional and teaching me all the bases to accomplish this work.

CONTENT

LIST OF FIGURES

LIST OF TABLES

LIST OF APPENDICES

RESUMEN

Título: Caracterización Geométrica y Temporal del Corazón utilizando la transformada Densa de Hough en CMR [1]

Autor: Jean Alejandro Pico Velásquez[2]

Palabras Clave: Corazón, Transformada Hough, Descriptor, CMR, MRI, Imágenes Biomédicas, Caracterización, Segmentación cardíaca, Predicción de enfermedades cardíacas

DESCRIPCIÓN:

El desarrollo y la propuesta de herramientas de apoyo al diagnóstico y la monitorización de las patologías cardiacas son esenciales para ayudar a los médicos en la rutina clínica. Sin embargo, la caracterización del corazón es una tarea muy compleja debido a la alta variabilidad geométrica y dinámica de sus estructuras. Adicionalmente, la resonancia magnética (MRI) en la rutina clínica tiene restricciones temporales y espaciales que limitan el análisis observacional de este órgano en particular. El objetivo de este trabajo es proponer un descriptor espacio-temporal que permita la caracterización no paramétrica de estructuras cardiacas utilizando la transformación Dense Hough (DHT). Este trabajo involucra la evaluación multi-escala de secuencias de resonancia magnética cardiovascular (CMR), así como el análisis de primitivas de movimiento y deformaciones que pueden ser codificadas en tablas acumulativas para lograr una representación robusta. Las estructuras cardíacas se codificaron a partir de la DHT y se implementaron en dos escenarios diferentes: segmentaciones del ventrículo derecho y clasificación automática de la enfermedad. En la primera tarea, para la segmentación del ventrículo derecho, la estrategia propuesta logró una precisión de 0.87 en un conjunto de 95 muestras. Para la segunda tarea, el reconocimiento de las enfermedades del corazón alcanza los 70.7% de precisión en un conjunto de datos con cuatro patologías diferentes.

---

[1] Trabajo de Grado

[2] Facultad de Ingenierías Físico-Mecánicas. Escuela de Ingenierías Eléctrica, Electrónica y de Telecomunicaciones. Director: Fabio Martínez Carrillo, PhD.

ABSTRACT

Title: Geometric and Temporal Heart Characterization using Dense Hough transform in cardiac MRI[1]

Author: Jean Alejandro Pico Velásquez[2]

Keywords: Heart, Hough transform, Descriptor, CMR, MRI, Biomedical imaging,, Characterization, Cardiac Segmentation, Cardiac disease prediction .

DESCRIPTION:

The development and proposal of tools to support the diagnosis and monitoring of cardiac pathologies are essential to assist physicians in clinical routine. Nevertheless, heart characterization is a very complex task due to the high geometric and dynamic variability of their structures. Additionally, magnetic resonance imaging (MRI) in clinical routine has temporal and spatial restrictions that limit the observational analysis of this particular organ. This work aims to propose a spatial-temporal descriptor that allows non-parametric characterization of cardiac structures using Dense Hough transform (DHT). This work involves multi-scale evaluation of cardiovascular magnetic resonance (CMR) imaging sequences, as well as analysis of motion primitives and deformations that can be coded in cumulative tables to achieve a robust representation. The heart structures were coded from DHT and implemented in two different scenarios: right ventricle segmentations and automatic disease classification. In the first task, for right ventricle segmentation, the proposed strategy achieved 0.87 of accuracy in a set with 95 samples. For the second task, the recognition of heart diseases achieves 70.7% of accuracy in a dataset with four different pathologies.

---

[1] Bachelor Thesis

[2] Faculty of Physics-Mechanics Engineering. School of Electric, Electronic and Telecommunications Engineering. Advisor: Fabio Martínez Carrillo, PhD.

INTRODUCTION

Cardiovascular diseases (CVD) are the main cause of death around the world, according to the World Health Organization (WHO). In clinical routine, the analysis of the cardiac cycle from sequences of Magnetic Resonance images (cine-MRI) is crucial for the evaluation of the functionality of the heart in anatomical terms, thus supporting the diagnosis and prognosis of such diseases [1]. Quantitative heart patterns estimation is, however, challenging [2] since the success of this examination depends entirely upon the observational skills of the expert physician, with the inevitable inter and intra-observer variabilities. For instance, the delineation of cardiac structures can take more than 15 minutes for each patient while being susceptible to inter-expert variability [3].

The development of CAD (computer-aided diagnosis) systems that help physicians in detection, diagnostic and following of heart diseases is essential to support standard clinical protocols. For instance, the characterization of structural and dynamic heart patterns could be relevant to reduce ambiguity in diagnosis. Also, such characterization could help physicians with a tedious task such as the delineation of ventricles or the computation of volumetric spatio-temporal patterns [4, 5]. The development of such tools is, however, a challenging task because of the structural and dynamic complexity of the heart that deforms dramatically along the cardiac cycle [6]. Regarding motion, the non-linear performance of the heart is observed as large displacements. Such fact results from a low temporal resolution of cine-MRI and increases the difficulty in the development of analytical tools to analyze the heart.

Two main tasks are being implemented and developed to help the physician in the routine of cardiac analysis: ventricle segmentation and cardiac pathologies prediction based on examples. For the first task, many strategies have been explored in the literature to segment the left ventricle [7, 8, 9] due to its importance in the quantification of

volumetric patterns associated with some cardiac diseases. Nowadays, it is well known that right ventricle (RV) characterization is also fundamental to compute volumetric patterns that help with diagnostic decisions[3, 10, 11]. The purpose of segmentation is to help with the characterization of specific diseases, such as pulmonary hypertension, cardiomyopathy, myocardial infarction, and congenital heart disease. The RV segmentation task is still an open problem in the scientific community because of the high variability between different cardiac MRI volumes, the complex shape of RV and the presence of trabecular muscles in the cavity which have similar gray-scale values as the surrounding myocardium.

Particularly, the automatic segmentation of the right ventricular has been explored from different statistical models that include priors of appearance and structure that match the shape of a set of samples [12, 13]. These models, in general, identify RV contours by minimization of non-common data between the model and the image. Nevertheless, this method lacks robustness due to RV variability across different slices, frames, and patients. On the other hand, atlas-based segmentations are proposed in the literature as an alternative to segment the RV. These strategies impose anatomical priors from a set of samples, allowing to cover the structure of RV globally at the expense of local description capabilities. In such way, these methods overcome noise and low tissue-to-blood contrast problems. Regarding prior overlapping, there are different alternatives. These use the most similar sample from a training set and also the multi-atlas approaches that cover a general model that is registered to a target [14, 15].

Regarding the second task, prediction based on a set of labeled cine-MRIs, a set of samples that have been previously annotated by an expert is used to suggest a cardiac pathology in a new sample. In the literature, different techniques have been proposed that aim to characterize both morphologically and physiologically the heart by using different computational strategies that range from appearance descriptors, edge ventricle estimation and quantification of motion. For instance, in [4] they computed the global heart orientation path along cardiac cycle to identify pathologies. Such approach is however very sensitive to large displacements. In [16], they proposed to combine learning algorithms with deformable models to automatically segment and detect heart patterns. This approach obtains good results regarding accuracy but with a considerable computational cost. Khemphila [17] *et. al.* proposed a heart pathology classification strategy from a deep neural network. This computational approach

nevertheless requires a large training data, which implies high computational cost, a critical point in clinical protocols.

This work aims to propose a heart characterization by using a Dense Hough transform which allows analyzing non-rigid structures. The dense characterization was applied in two different scenarios: RV segmentation and automatic classification of pathologies. In general, the proposed Hough descriptor is computed at different cine-MRI slices at different scales. From an initial delineation of the structure of interest, the proposed approach can track the regions of interest along the cardiac cycle. Then, for the first scenario, the detected Hough region is included in a probabilistic approach to obtain a shape approximation of right ventricle. In a second scenario, the Hough Dense representation is used to detect several cardiac regions of interest that are characterized by the motion field computed in these areas. Then a machine learning strategy is used to classify the different motion descriptors obtained.

Chapter 1
METHODOLOGY

In this work, a low-level heart representation is achieved by using a special Dense Hough Transform (DHT). This transformation is operated pixel-wise into a multi-scale scheme that allows following non-parametric shapes along time. From such local representation, it is possible to characterize cardiac structures that exhibit complex spatial and temporal performances. Following the main assumption of this thesis, the DHT was used as the main reference to track and detect cardiac regions that were subsequently analyzed into two different scenarios, described as follows:

- **Right Ventricle (RV) Segmentation.** This was the main scenario explored in this work. In this case, the DHT allows to detect and follow a region that bound the right ventricle. Then a probabilistic model is herein implemented to segment RV from the background. At each time, the DHT and probabilistic model are complemented and updated to achieve a temporal segmentation. A complete description of this scenario is developed in subsection 1.2.

- **Classification of Heart Diseases.** The DHT was also successfully applied to a cardiac disease classification problem. In such case, the DHT characterization of heart allows to code information independently from both chambers: left and right ventricles, as well as the detection and tracking of heart along the cardiac cycle. Each of detected regions was locally coded with motion histograms to carried out a description of particular heart dynamics. The obtained descriptor was mapped to a previously trained support vector machine to obtain a disease prediction. A full description of this scenario is in Appendix A.1.

1.1 Dense Hough Transform (DHT) for heart characterization

In this section, we will detail the main contribution of this degree project, which, as indicated by the main objective, consisted of the characterization of the heart using DHT. More specifically, the objectives: Local Characterization (Section 1.1.1), Heart Detection (Section 1.1.2), Heart Tracking (Section 1.2.2 and 1.2.3) and Validation of the proposed heart characterization in two scenarios (Section 2 and Appendix A.1). The particularities of this representation will be detailed below.

A cine-MRI captures the heart structures together with surrounding organs along the cardiac cycle. A fundamental task is to obtain a representation of the cardiac structures over time, allowing to identify and track these regions automatically from others in cine-MRI. In this work, an initial delineation of cardiac structures is taken at the first slice, and then a Dense Hough representation allows to detect and follow the marked regions of interest (RoIs). Hence, a template $\zeta_{\mathbf{x}}$ is computed over a rectangle surrounding RoIs, centered at position $\mathbf{x}$. Since an MRI sequence is a temporal volume, such template can be computed at every slice where cardiac structure exists or can be computed at independent slices of importance for the analysis (e.g., the basal, mid and apical slices). The characterized template is then used to search and detect the respective RoIs in the whole slice for all cine-MRI volumes.

1.1.1 Learning: $\zeta_{\mathbf{x}}$ representation Let be $\mathbf{x}$ a pixel location with coordinates x, y. The template is characterized by means of a multi-scale framework $\{\zeta^{\sigma}_{\mathbf{x},\mathbf{i}} = \zeta_{\mathbf{x}} * \left(\frac{\partial G_{\sigma}}{\partial \mathbf{x}^i}\right)\}$, that essentially exploits the spatial structure and features provided by the first and second derivatives at different scales $\sigma = \{\sigma_1, \ldots, \sigma_n\}$. This multi-scale approach probed to reduce the influence of spurious structures, which improved detection [18]. From such template $\zeta^{\sigma}_{\mathbf{x},\mathbf{i}}$ is possible to compute local primitives at each location $\mathbf{x}$ such as the curvature $\kappa_{\mathbf{x}}$ (as Eq. 1.1) and gradient orientation $\theta(\nabla\zeta_{\mathbf{x}_\mathbf{i}})$ (Eq. 1.2) [18].

$$\kappa_{\mathbf{x}} = \frac{\zeta_{xx}\zeta_y^2 - 2\zeta_{xy}\zeta_y\zeta_x + \zeta_{yy}\zeta_x^2}{||\nabla\zeta_{\mathbf{x}}||^3} \tag{1.1}$$

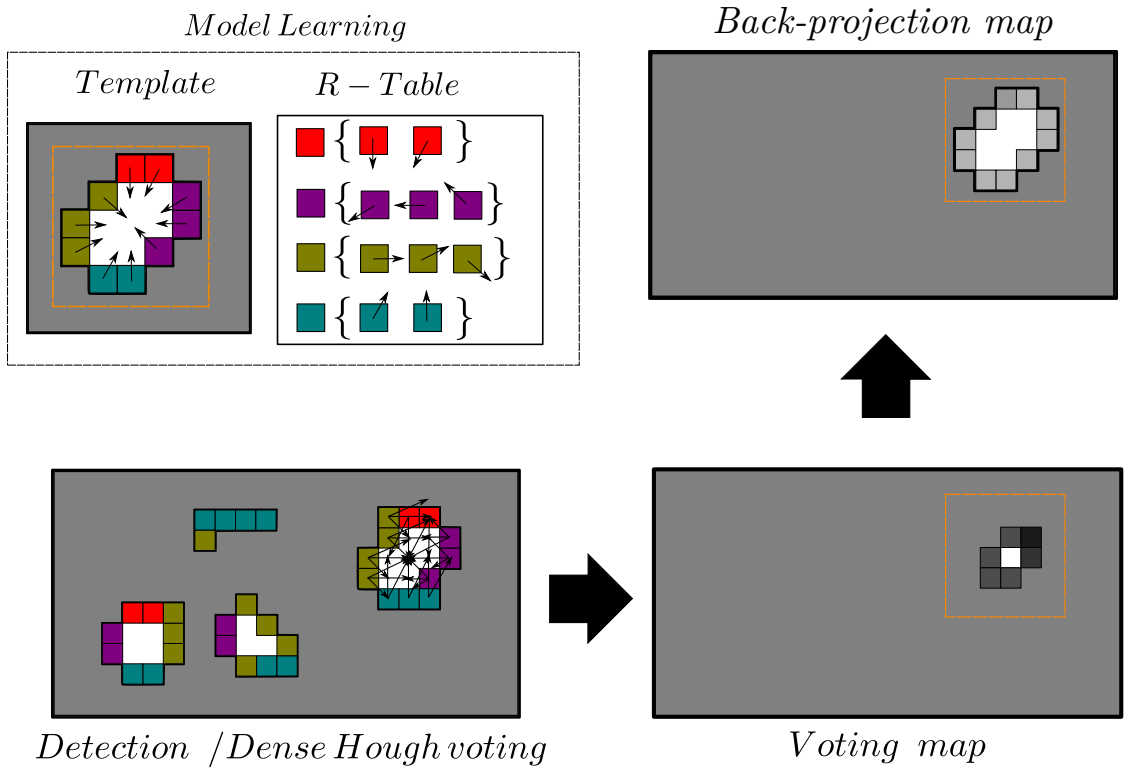

Figure 1. Automatic Right Ventricle Detection.

$$\theta(\nabla\zeta_{\mathbf{x}}) = \begin{cases} \pi + \tan(\frac{\zeta_y}{\zeta_x})^{-1}, & \text{if } \zeta_x\zeta_y < 0. \\ \tan(\frac{\zeta_y}{\zeta_x})^{-1}, & \text{otherwise.} \end{cases} \tag{1.2}$$

From such multi-scale representation, it is possible to perform a more robust search in the next frames to detect the cardiac structures of interest. For doing so, two representation tables (RT_n) were defined as accumulators arrays that count occurrences of gradient orientation ($\theta_{\mathbf{x}}$) and curvature ($\kappa_{\mathbf{x}}$) for each pixel, respectively. To limit its size these features are quantized and the curvature is bounded to $[-1, 1]$. For RTs calculation those pixels with a gradient magnitude equal to 0 are bypassed, avoiding non defined value estimations. The algorithm 1 shows systematic construction of the two R-tables. In such case, $RT_1(\theta(\nabla\zeta_{\mathbf{x_i}}), \sigma)$ concatenates weighted gradient orientations and relative positions ($\Delta_{\mathbf{x}}$) w.r.t the center. $RT_2(\kappa, \sigma)$ += $(\Delta_{\mathbf{x}}, ||H_{I\mathbf{x}}||)$ concatenates information with respect to the curvature index and by the Frobenius norm of the Hessian matrix.

Algorithm 1 Algorithm for template learning from the Dense Hough transform. First and second order spatial features are used to create representation tables (RTs) for the first frame in each slice in MRI volumes. These tables are updated during each slice sequence (See subsection 2.2.2).

Require: Gray-scale image template
Ensure: RT_1,RT_2 $\rightarrow$ Representation tables
1: **for** all pixels $\mathbf{x}$ $f_i^\sigma : \{\theta^\sigma, \kappa^\sigma\}$ **do**
2: Compute$\{\theta^\sigma, \kappa^\sigma, \nabla I^\sigma, ||H_I||_F^\sigma\}$
$RT_1(\theta(\nabla\zeta_{\mathbf{x_i}}), \sigma)$ += $(\Delta_{\mathbf{x}}, ||\nabla I_{\mathbf{x}}||)$ $RT_2(\kappa, \sigma)$ += $(\Delta_{\mathbf{x}}, ||H_{I\mathbf{x}}||)$
3: **end for**

Figure 2 illustrates the characterization process for a cardiac structure of interest, e.g., the right ventricle (RV). In this case, all pixels inside the rectangular RoI are considered the template for learning. This process is done once for each MRI volume, during the following frames these RTs are updated by adding the RV structural changes over time.

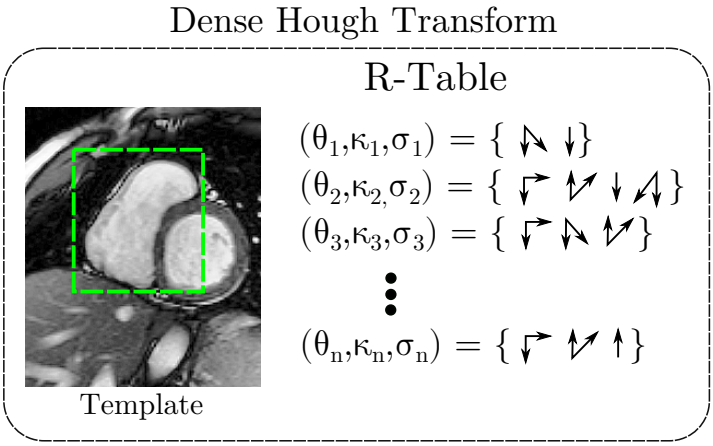

Figure 2. Basal slice: RV characterization example using a rectangular RoI Ω_{dht} for learning

1.1.2 Detection: searching $\zeta_{\mathbf{x}}$

From such local RoI characterization is possible to detect arbitrary non-analytical tissues such as the ventricles. Each RT is then projected into each new slice for search similar features and built an accumulation map (Γ). Every pixel vote according to its orientation and curvature indexes and its votes are weighted as indicated in the RT. The local maximum in the accumulation map is then considered as the center of detected RoI. Algorithm 2 summarizes the automatic detection of RoIs for every slice at each cine-MRI of the dataset.

Figure 3 shows the accumulation map calculated from a cine-MRI. Where the brightest

Algorithm 2 Algorithm to search the *RoI* template in a new slice from the dense Hough transform. The RTs are mapped into the new cine-MRI, and an accumulation map is built as the likelihood of each template w.r.t the image region.

Require: Gray-scale image / RT_1 / RT_2
Ensure: $\Gamma \rightarrow$Accumulation map
1: **for** all pixels $\mathbf{x}$ $f_i^\sigma : \{\theta^\sigma, \kappa^\sigma\}$ **do**
2: Compute$\{\theta^\sigma, \kappa^\sigma, \nabla I^\sigma, ||H_I||_F^\sigma\}$
3: **for** $(\Delta_\mathbf{x}, w)$ in $RT_i(\sigma, f_i^\sigma)$ **do**
4: $\Gamma(\mathbf{x} + \Delta_\mathbf{x}) \mathrel{+}= w$
5: **end for**
6: **end for**

pixel at position $\mathbf{x}$ represents the RV center with some margin of error. This voting map is computed over the time for each frame and each slice.

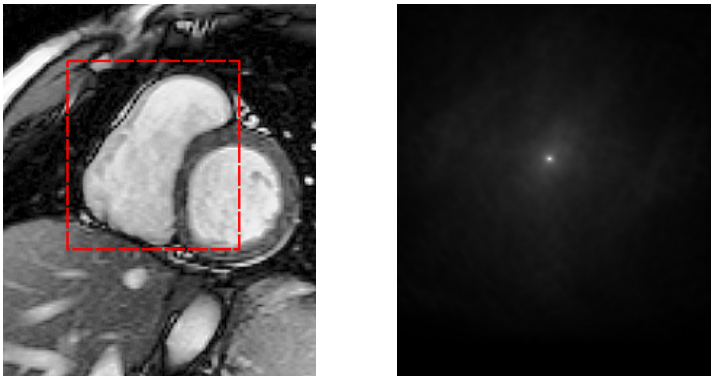

RV Detection Voting map

Figure 3. **Left:** RV RoI detected for a Basal slice, **Right:** Accumulation map which represents the voting process for detection.

1.1.3 Back-projection

From the voting map, it is possible to recover the center of the estimated RoI $\hat{\zeta}_\mathbf{x}$ along the cardiac MRI-sequence. Then, at each time is possible to obtain an automatic identification of the selected structure. Additionally, a local contribution of each pixel can be recovered from the voting map. From such assumption, the pixels that better represent cardiac structures have significant contributions to the voting map. In this sense, a rough non-parametric shape can be recovered from the voting map by selecting the pixels with significant contributions [19]. In segmentation scenario, a back-projection strategy is implemented from a thresholded version of contributing pixels. This coarse model is used to update the segmentation model that

leads to better discrimination of foreground and background pixels into the region of interest.

1.2 First scenario: Right Ventricle Segmentation

The Right Ventricle structure and function plays an essential role in diagnosing and monitoring many cardiovascular diseases. Nevertheless, the complex dynamic a non-parametric shape of RV difficult the task of segmentation. In this section, it is proposed an automated RV segmentation method by characterizing the region with the DHT and then including a statistical framework of classification.

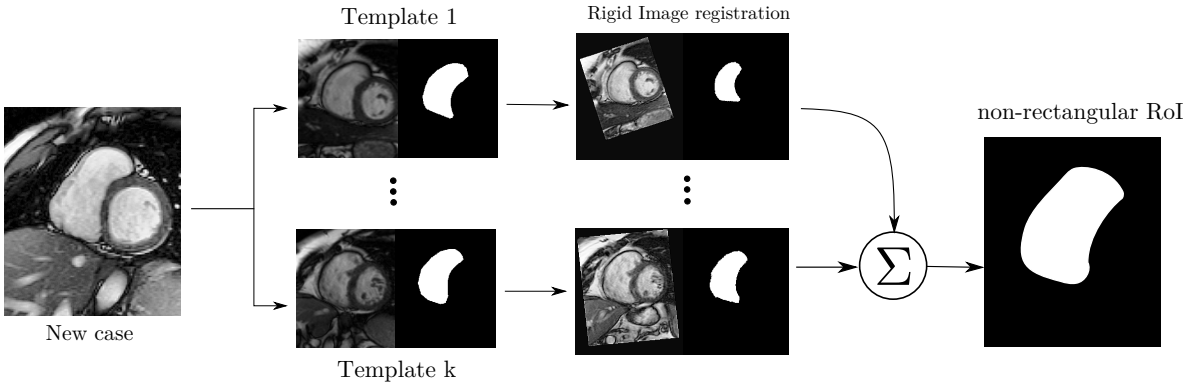

Figure 4. **Automatic non-rectangular RoI estimation**. First, the dataset volumes are rigid registered w.r.t the target (New case). Then, all contours are transformed to fit the target. Finally, an average between all contours is computed to obtain a non-rectangular RoI estimation (Ω) for the new case.

The proposed method starts by automatically estimating the region of interest, that corresponds to an RV approximation. For doing so, a rigid registering strategy is herein used to avoid undesired deformations in the Right Ventricle morphology. Hence, like an atlas-based approach, a dataset with contours given by a physician expert is registered with respect to a new case without them. Each contour is transformed accordingly to its corresponding MRI volume. Finally, a non-rectangular RoI (Ω) is estimated according to a transformed contours average: $X_{avg} = \frac{1}{N}\sum_{i=1}^{N} X_i$ of samples in training. In Figure 4 is illustrated the process of rigid registration of a set of training samples with respect to a target. The initial delineation, taking from average is then characterized with the DHT an evolved according to a statistical framework as described as follows.

1.2.1 Probabilistic Segmentation model

Once the Hough representation is recovered, the main scenario for evaluation was heart chambers segmentation. For doing so, the Hough transformation is complemented with a probabilistic approach. The heart shape estimation S_t is involved in a well defined cardiac cycle description $S_t, \rightarrow S_{t-1} \rightarrow S_{t-2} \ldots$, where consecutive shape evolutions depend on temporal motion and deformation history. Additionally to history information, at each time t, it is possible to recover a particular observation of heart $\hat{S}_{t-1} = S_{t-1} + \mathbf{e}$, where $\mathbf{e}$ represents noise in the captured measurements. From such analysis, it is can approximate the heart dynamic segmentation as a Bayesian inference of first order, described by Chapman-Kolmogórov equation :

$$p_{ij}^{n} = \sum_{k=0}^{M} p_{ik}^{m} \, p_{kj}^{n-m}$$

where p_{ij}^{n} represents the transition probability from state i to state j in n steps or iterations. For our case, it is assume that heart chambers do not change their shape between frames abruptly. In this assumption, it is consider a Markovian first approximation, *i.e.*, the most important information of motion history is in the previous frame $(t-1)$.
Like in [19], a segmentation model is adopted which is trained and updated during the cardiac cycle to improve discrimination. For this segmentation model, a recursive Bayesian formulation approach is used, based on tissue-to-blood contrast present in the RoI in a time t. The Bayesian inference allows to increase model robustness by incorporating the information present in previous sequences $(t-1)$. To create this model, two probabilities are defined for each position $\mathbf{x}$, that is, probability of the pixel $\mathbf{x}$ to belong to RV (Foreground) and probability of the pixel $\mathbf{x}$ to be any other tissue (Background). Let $C_{t,\mathbf{x}}$ be the pixel class at the position $\mathbf{x}$ at a time t. Where $C_{t,\mathbf{x}} = 0$ for surrounding tissues and $C_{t,\mathbf{x}} = 1$ for RV. Furthermore, be $y_{1_t,\mathbf{x}}$ the tissue-to-blood contrast information in the position $\mathbf{x}$. The probability of the pixel $\mathbf{x}$ pertaining to the right ventricle ($P(C_t = 1|y_{1:t})$) is defined by:

$$p(c_t = 1|y_{1:t}) = \sum_{c_t - 1} p(y_t|c_t = 1)p(c_t = 1|c_{t-1})p(c_{t-1} = 1|y_{1:t-1}) \tag{1.3}$$

Let Ω be the RoI obtained in Figure 4. From Ω, two scaled version are created $(\Omega_{fg}, \Omega_{bg})$. For the first case $(\Omega_{fg} = 1.3 * \Omega)$ the inner region is taken, which contains the pixels corresponding to RV. In the second case, the region resulting from the difference between

$1.5 * \Omega$ and Ω_{fg} i.e. $\Omega_{bg} = 1.5 * \Omega \; xor \; \Omega_{fg}$ (See Figure 5) is taken.

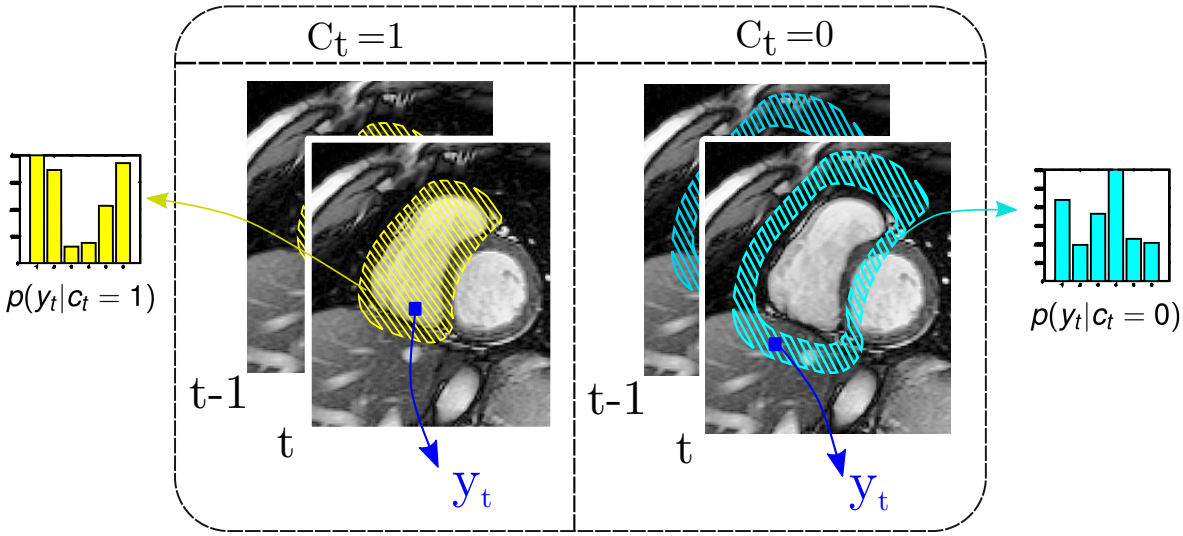

Figure 5. **Left:** Foreground area Ω_{fg} where RV histogram is calculated; **Right:** Background area Ω_{bg} where surroundings tissues histogram is calculated

Once Ω_{fg}, Ω_{bg} are obtained, color histograms are calculated into these regions, which are normalized and quantized at 12 and 24 bins per region. These histograms contain the tissue-to-blood contrast information necessary for the construction of the model based on Bayesian inference.

A prior $P(C_t = 1)$ is initialized in Ω_{fg}. Hence, the resulting $P(C_t = 1|y_{1:t})$ can be observed in Figure 6. Thus, the final segmentation is obtained by thresholding this RV probability image (see Figure 6-(b)(d)). Being the best performance value $\tau = 0.2$ as shown in Figure 11.

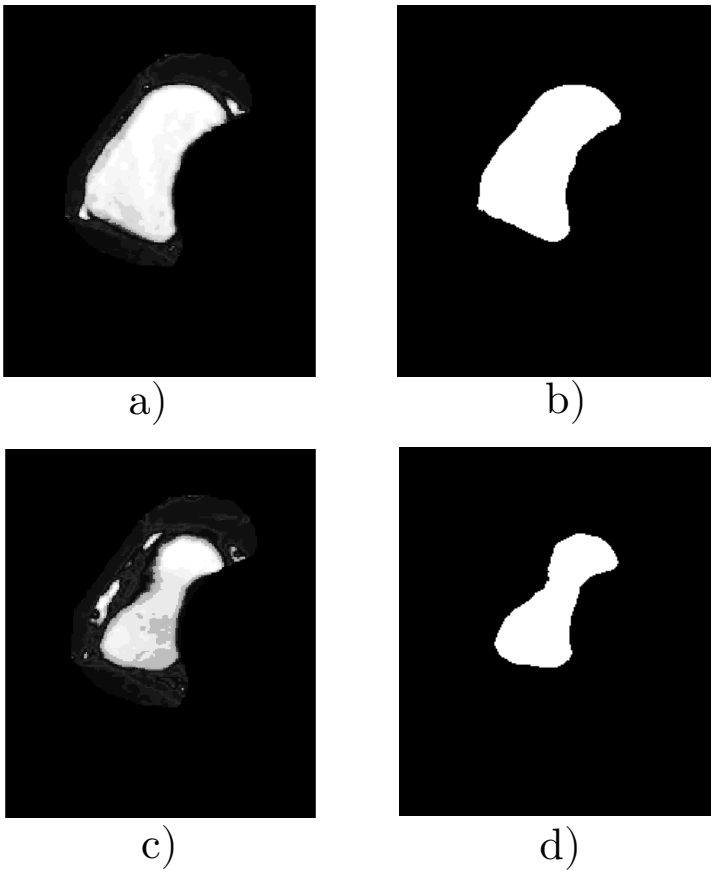

Figure 6. **Segmentation model**. **a)** Diastole RV probability; **b)** Diastole segmentation; **c)** Systole RV probability; **d)** Systole segmentation

1.2.2 Tracking In a new frame corresponding to the same MRI sequence, the automatic detection and segmentation are calculated within a RoI Ω. In this way, the new position of the RV (X_t) can be re-evaluated. To improve the robustness in the estimation of the ventricle position due to changes in its morphology (non-rigid deformations); not only is the Dense Hough transform output used, (X_{dht}), i.e. the local maximum of the voting map (Γ), but also the segmentation in the previous frame is used. The center of mass of the segmentation is evaluated according to the equation 1.4

$$X_{seg} = \frac{1}{S} \sum_{x \in \Omega} P(C_t = 1|y)\, x \tag{1.4}$$

Where S is the sum of all the probabilities $P(C_t = 1|y) \in \Omega$. The new center of the object is estimated by a linear combination of the Hough detection output X_{dht} and the

center of mass X_{seg} of the segmentation . The α factor in the equation 1.5 adjusts the relevance, reliability or weight of either X_{dht} for small values or X_{seg} for values larger than α. Experimentally an α equal to 0.2 was selected.

$$X_t = \alpha X_{seg} + (1 - \alpha) X_{dht} \tag{1.5}$$

1.2.3 Model Adaptation

The segmentation and Dense Hough detection models are updated in a manner that complements each other, i.e., the upgrading of one model depends on the other. The Dense Hough model update recalculates the $\Delta_{\mathbf{x}}$ displacements within the rectangular RoI Ω_{dht} (Figure 2). In such case, the weights are then updated using the constraints shown in the equations below. Where if the $\Delta_{\mathbf{x}}$ displacements exist in the RT_n model their weight will be updated, otherwise, this displacement will be added to the corresponding RT_n table.

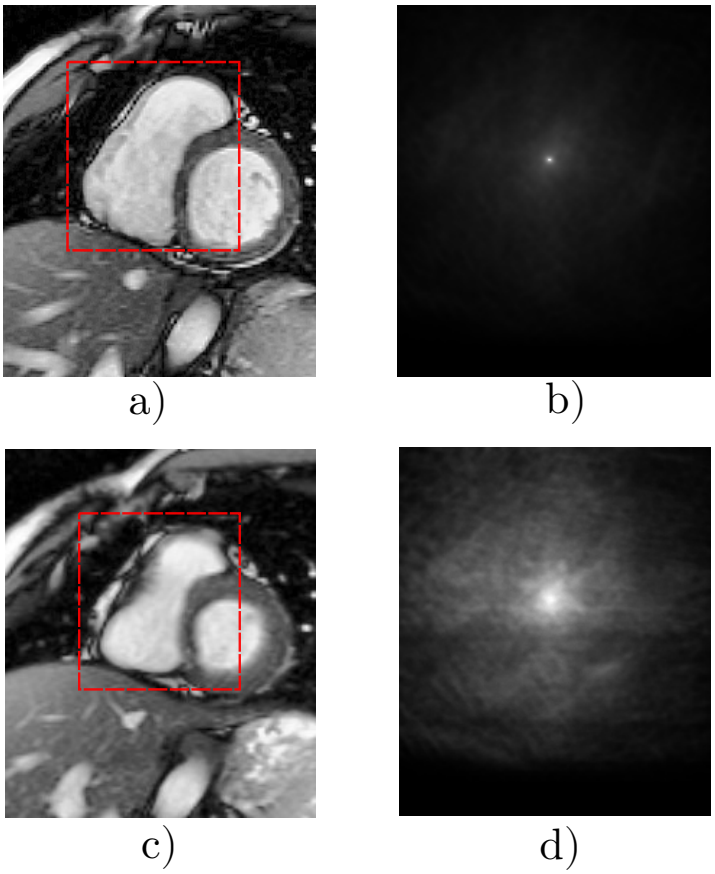

Figure 7. **Hough model updating**. **a)** Diastole cine-MRI; **b)** Diastole Voting map ; **c)** Systole cine-MRI; **d)** Systole voting map

$$w_1 = \begin{cases} \gamma P(C_\chi = 1|y)\, w_1 + (1-\gamma) w_1, & \text{if } \Delta_\chi \in RT_1(\theta, \sigma). \\ \gamma P(C_\chi = 1|y)\, ||\nabla I||, & \text{otherwise.} \end{cases}$$

$$w_2 = \begin{cases} \gamma P(C_\chi = 1|y)\, w_2 + (1-\gamma) w_2, & \text{if } \Delta_\chi \in RT_2(\kappa, \sigma). \\ \gamma P(C_\chi = 1|y)\, ||H_I||, & \text{otherwise.} \end{cases}$$

As RV has several deformations during the MRI sequence, the Hough descriptor (RTs) should take in the count this changes. In Fig. 7 is shown how the detection works for a critical scene where the RV has the maximum contraction (Systole). It is noticeable how the voting map became noisier but still detects the RV correctly. In this case, the model was trained for Diastole scenario.

The segmentation model updating uses back-projection map information to update the histograms for RV and non-RV tissues. For this, only pixels with vital importance or significant influence in the voting map maximum are take in the count. In our case, only greater than 0.5 (In a range from 0 to 1). These pixels increase their importance in the probability model, while the others decrease (as shown in the equation below). Turning into better discrimination. Empirically an update factor $\delta = 0.1$ was chosen.

$$P(y_t|c_t = 1) = \delta\, P(y|b > 0.5) \; + \; (1-\delta) P(y_{t-1}|c_{t-1} = 1)$$

Chapter 2
EXPERIMENTS AND RESULTS

The proposed heart characterization was evaluated in two different scenarios. In both cases were used real public datasets of cine-MRIs sequences. Also, were used common cross validation frameworks to validate the results in specific applications. A full description of obtained results are described in next subsections:

2.1 First scenario: Right Ventricle Segmentation

In this section, the proposed method was evaluated was evaluated in the RV-segmentation problem. As described in methodology, the DHT was included in a statistical framework to obtain an estimation of the right ventricle. The implementation of the algorithm was written in MATLAB 2018a and run over a standard PC of 64 bits in an Intel Core i5 processor (4 Cores @3.2GHz) and 8Gb of RAM with Ubuntu 16.04.
The evaluation of the proposed RV Segmentation was performed over the Right Ventricle Segmentation Challenge (RVSC) dataset which was organized by MICCAI'12 [3]. This consists of a total of 16 patient short-axis volumes and a set of ground truth contours. All patients' data were anonymized according to the MICCAI'09 LV segmentation challenge criteria [3]. The CMR study was performed at 1.5T Symphony Tim, Siemens Medical Systems. A conventional 2-chamber view was acquired with a total of 10-14 short-axis slices from Apex to Basal. The examination parameters were the following: TR = 50 ms; TE = 1.7ms; flip angle = 55; slice thickness = 7 mm; matrix size = 256 216; Field of view (FOV) = 360 mm 420 mm; 20 images per cardiac cycle [3]. Manual delineation was carried out by an expert cardiologist who manually delineated endocardial and epicardial contours of the RV. As suggested by dataset authors, two different metrics were herein used to evaluate the performance of the proposed ap-

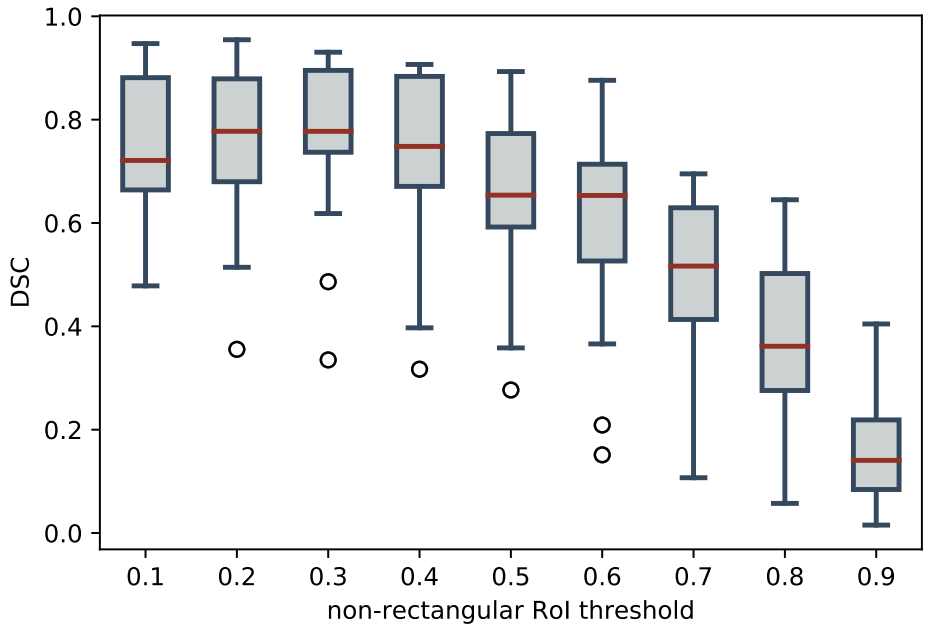

Figure 8. Influence of non-rectangular RoI threshold parameter.

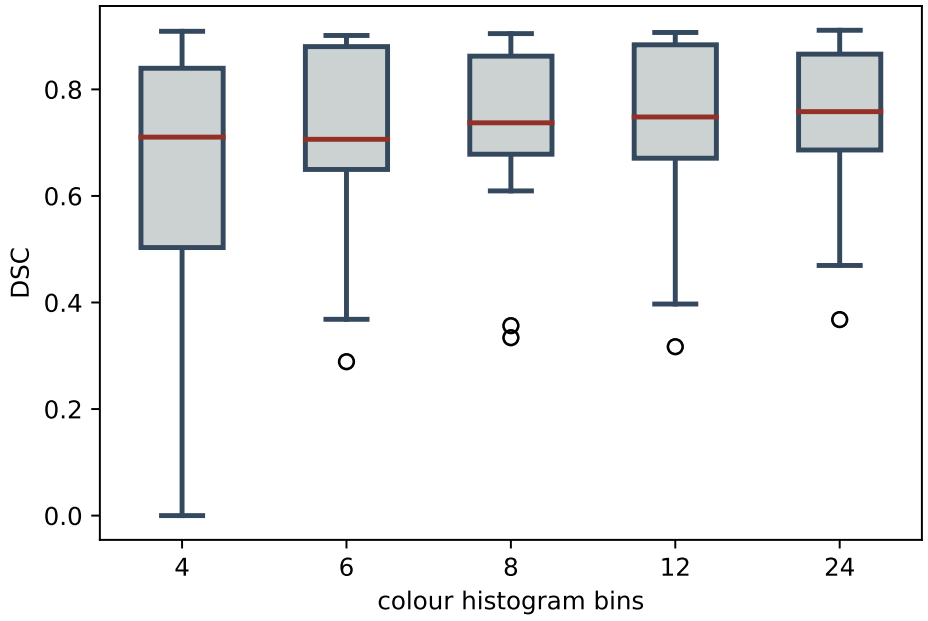

Figure 9. Influence of colour histogram bins parameter.

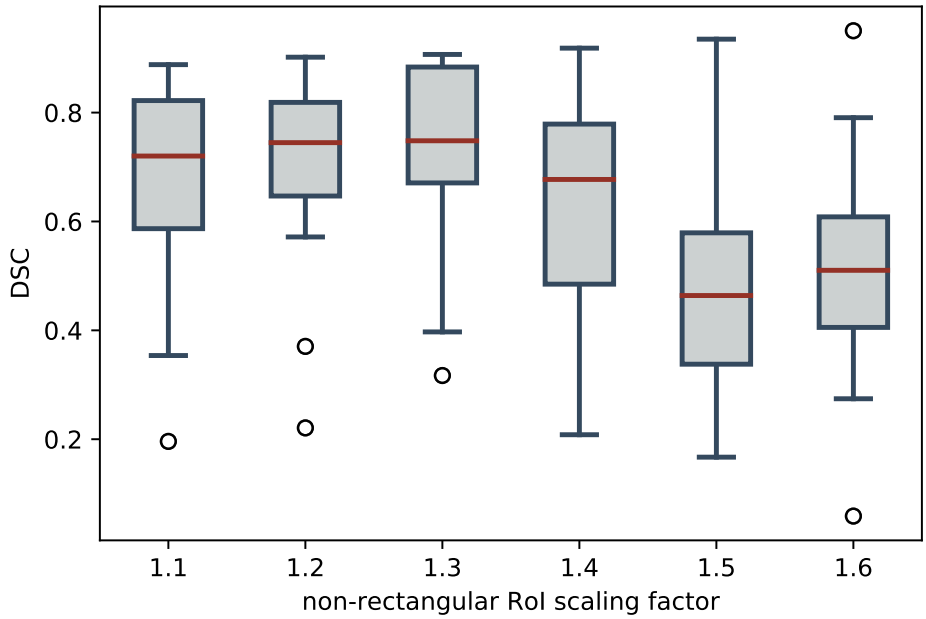

Figure 10. Influence of non-rectangular RoI scaling factor parameter.

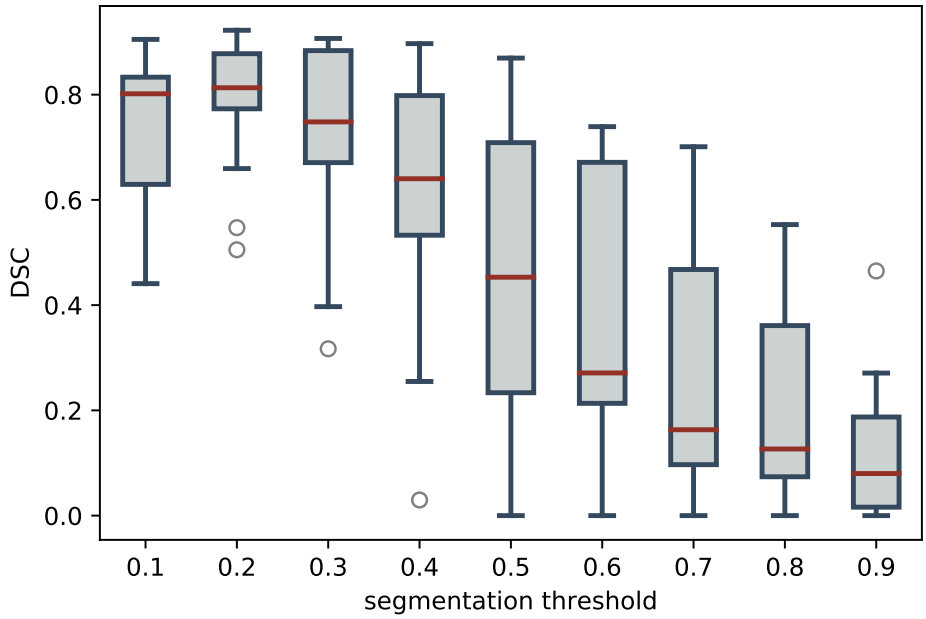

Figure 11. Influence of segmentation threshold parameter.

proach: The global Sørensen–Dice coefficient (DSC) and the local Hausdorff Distance (HD). On the one hand, the similarity Sørensen–Dice coefficient computes the spatial overlap between two discretely labeled objects. It is a traditional metric for segmentation performance evaluation, where the similarity between the ground truth (GT) and the RV segmentation is measure in a range from 0 to 1 (higher is better), described as: $DSC = \frac{2(GT \cap RV_{seg})}{GT + RV_{seg}}$. On the other hand, the Hausdorff Distance (HD) measures how far two contours are from each other. Hence, this metric gives us complementary information of similarity between A and B. Defined as: $HD(A, B) = \max_{a \in A}\{ \min_{b \in B}\{ d(a, b)\}\}$.

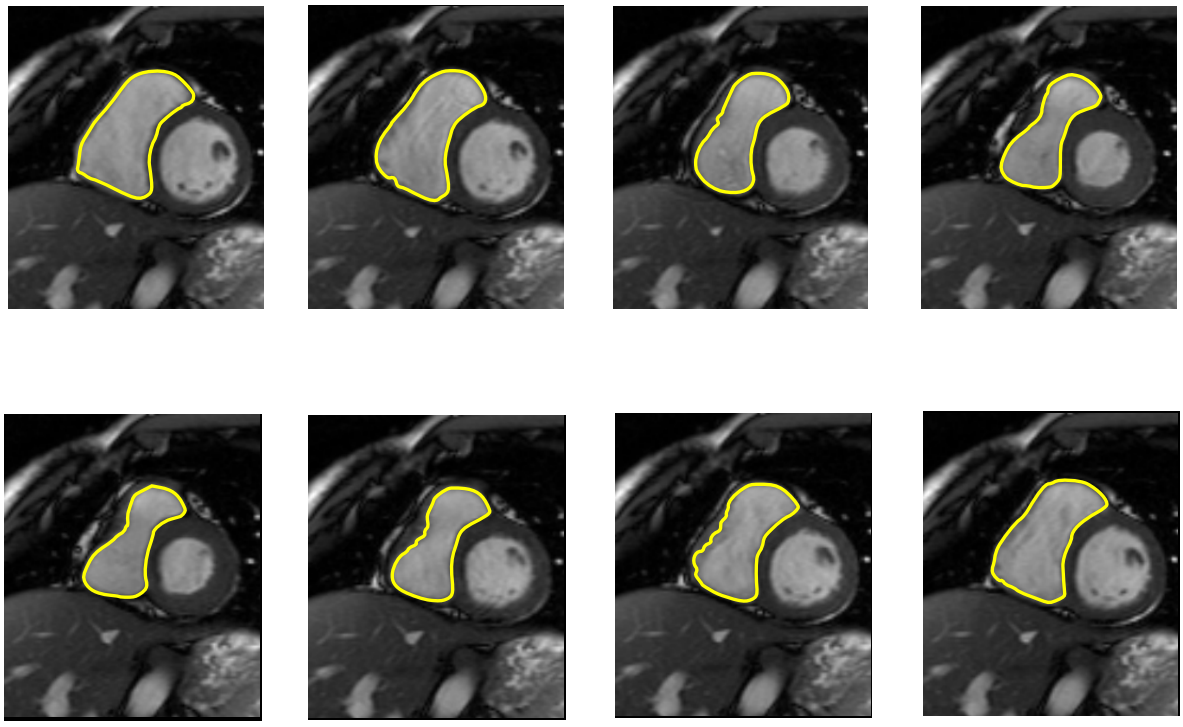

Figure 12. **Segmentation results for patient #4 during cardiac cycle. Yellow:** proposed RV segmentation

Firstly, a qualitative evaluation of obtained RV segmentations is illustrated in Figure 12, 13. In such cardiac cine, MR short-axis images can be observed the very well performance of the proposed strategy in basal heart regions, being very close to expert manual delineations. Also, for different shapes, the strategy is well adapted during the cardiac cycle (Figure 12). The approach is capable of following and tracking the RV motion and deformation. For apical images, Figure 13 second row, the region segmentation is much more challenge because the small regions where the RV-region is

present. Even for an expert physician, these slices are tough to segment. Nevertheless, the proposed approach achieves an appropriate segmentation in this apical regions with some local limitations.

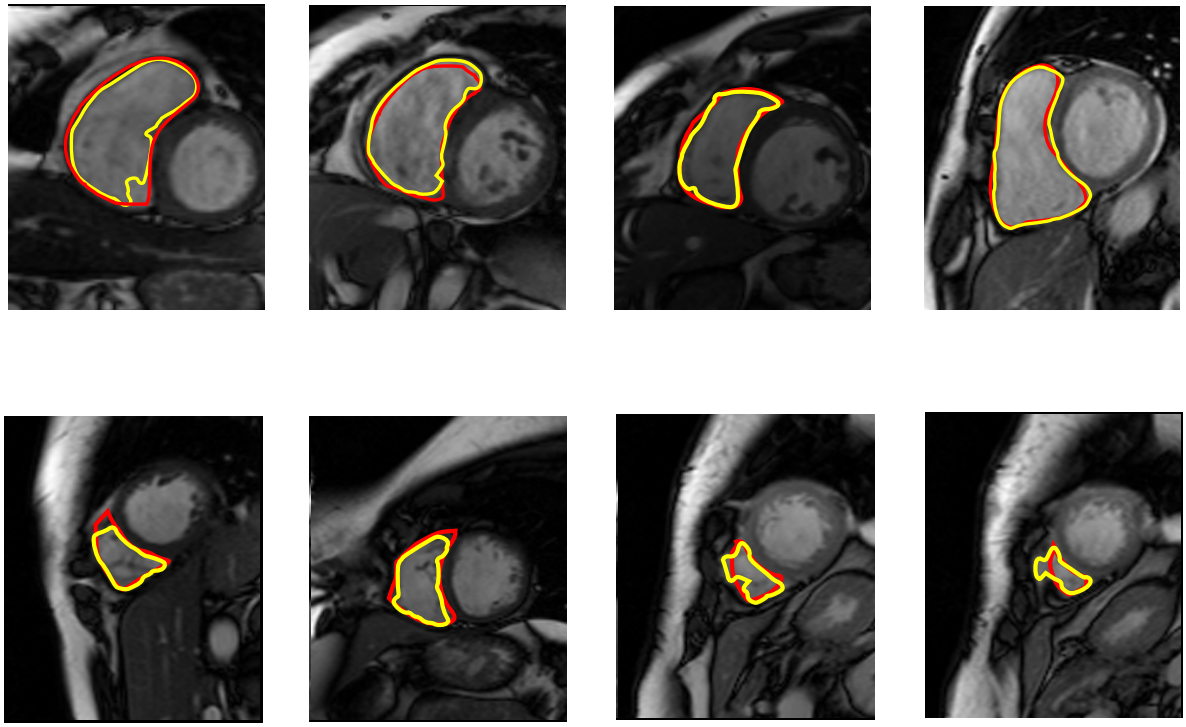

Figure 13. **Segmentation results from Basal to Apex. Yellow:** proposed RV segmentation; **Red:** ground truth contour

Secondly, an exploration was carried out to adjust the proposed approach w.r.t to parameters that are sensitive to the segmentation (see Figures 8, 9, 10, 11). The selected parameters evaluated in a spectrum of values are: non-rectangular RoI threshold, non-rectangular RoI scaling factor, color histogram bins, prior initialization, transition probability and segmentation threshold, described as follows:

- **non-rectangular RoI threshold:** That is applied to the average image contour obtained from the rigid registration. The threshold values are fixed in an interval between [0-1]. For values close to zero, a significant area of common delineations is taken into account while for values close to one only common values in whole delineations are considered. In Figure 8, that a value of 0.3 yields the best performance and less data variability, with an average accuracy of 0.81. In such

case, the proposed approach is better when is possible to admit larger region to initialize the algorithm.

- **non-rectangular RoI scaling factor (FG/BG):** Is computed to define the size of foreground (FG) and background (BG) area sizes, following the relation $\frac{fg}{bg}$ (see Figure 5). As illustrated in Figure 9 the best result is obtained when background RoI scale is 0.2 times bigger than the foreground. Statistically, such fact has sense since both regions are well equilibrated regarding samples to compute the histograms of each region.

- **colour histogram bins:** For quantization process necessary to build the tissue-to-blood contrast probability model. Specifically, Ω_{fg} and Ω_{bg} histograms quantization. In Figure 10 is shown that the performance remains almost constant for a different number of bins.

- **segmentation threshold:** Is applied to the RV image probability (Figure 6, Right). This is the final step for segmentation, which selects a set of pixels likely belonging to RV according to its probability of being RV. All pixels below the segmentation threshold are considered surrounding tissue. As expected, lower thresholds allow to take major information of RV area, leading to better performance of the proposed approach (see Figure 11).

In a third evaluation, the proposed approach was tested with three different configurations by coding different inputs delineations. Table with the result of these three different configurations is shown in Table 1. In a first case was only passed a rectangular region without any prior information of the heart shape (Fully rectangular). Interestingly, the proposed approach achieves in average an 88% of accuracy in basal, discovering by itself the true shape of the ventricle by only using appearance information. A second approximation takes into account the information of an initial delineation but computing the DHT overall region. As expected the result is much better because of the initial consideration of shape. Finally, the best result is achieved when the segmentation model is also updated w.r.t to the information of DHT at each time. Therefore, the model combines rectangular regions for detection and non-parametric regions for segmentation and updating. It is worth noting the improvement in apical slices by introducing properly prior knowledge of the training delineations.
In Table 2 is summarized the Dice Similarity Coefficient and Hausdorff Distance obtained by the proposed approach. A leave-one-out cross-validation was performed. For

Table 1. Quantitative comparison results for different RoIs approaches

RoI Approach	Basal	All slices
Fully Rectangular	0.88	0.66
Rectangular + Non-Rectangular v1	0.90	0.76
Rectangular + Non-Rectangular v2	**0.92**	**0.87**

Table 2. **RV Segmentation results;** Dice Similarity Coefficient (DSC) ± deviation standard. Hausdorff Distance (HD) average in pixels

	Measures	
	DSC (mean)	HD (mean)
Basal	**0.92 ±0.05**	4.19 ±1.54
All slices	0.87 ±0.12	**4.20 ±1.41**

this, a total of 16 patients with contours from RVSC dataset were used. The results were split for Basal and all slices (Basal, mid and apex). The best DSC were for Basal slices being around 0.92 on average with a low standard deviation. Both DSC and HD show a very compact performance of the obtained segmentation in global terms as well as the local description of RV shape. Nevertheless, the DSC decreases by around 0.1 from Base to Apex. In the state-of-the-art most methods perform DSC over 0.9 [20, 21, 22] for Basal slices. Additionally, adding apical slices decrease the DSC performance around 0.7. This indicates that increasing the segmentation performance for apical slices is a step forward. Most of the methods in the literature present problems with apex segmentation due to their appearance in MRI images, so creating models that do not rely fully on appearance for apical slices may improve the results. The segmentation error for apical slices is not considered a limiting factor for the volume calculation. However, it can be considered for other types of applications and studies. In comparison with inter-expert variability being 0.90 ±0.10 [3], for an automatic method, our results seem to have potential. Also, in comparison with LV segmentation state-of-the-art DSC is between 0.8 and 0.9 [7].

Finally, in Table 3, the accuracy of our proposed method was compared with the best results obtained in the Right Ventricle Segmentation Challenge (RVSC) at MICCAI'12 [3]. These methods use different approaches, such as 4D watershed graph-cut segmentation [23], 2D multi-atlas registration [24], 3D multi-atlas registration [25] and 2D shape

prior graph-cut segmentation [26]. Some of these methods need user inputs, i.e., are Semi-Automatic. For instance, (O. Maier et al.) [23] needs rough contouring of 4 to 5 2D slices.

Table 3. Metrics comparison with best methods presented in the Right Ventricle Segmentation Challenge (RVSC) MICCAI 2012. **All slices are considered**

Method	Self-reliance	DSC (mean)
Proposed approach	Automatic	**0.87 ±0.12**
CMIC (M. Zuluaga et al.)	Automatic	0.78 ±0.23
BIT-UPM (O. Maier et al.)	Semi-Automatic	**0.80 ±0.19**
ICL (W. Bai et al.)	Semi-Automatic	0.78 ±0.20
LITIS (D. Grosgeorge et al.)	Semi-Automatic	0.76 ±0.20

Chapter 3
CONCLUSIONS

In this work was introduced a local characterization of heart region over cine-MRI sequences. The characterization was achieved by computing a dense Hough transform (DHT) that allows to locally coded the region of interest by using angle and curvature primitives over each pixel. The implemented characterization result fundamental to understand how heart ventricle shapes changes over a cardiac cycle.

This dense cardiac Hough characterization was applied in two different scenarios: the Right ventricle segmentation and the automatic diagnosis prediction. In both scenarios the DHT result fundamental to follow non-parametric regions of interest and to coded relevant information of heart. In a first scenario, over a public dataset of 95 samples, the proposed strategy achieved an average score of 0.87. For second scenario, was evaluated the proposed strategy over a public dataset with four different pathologies. In such case, the proposed approach achieved an accuracy of 70.7%.

Futures perspectives include the use of additional local primitives to model the non linear heart performance in dynamic and shape. Also, additional evaluation will be carried out with more rich datasets. For instance in scenario 1: the left ventricle will be included to evaluate the performance of the proposed approach. In scenario 2: additional pathologies will be taken into account.

REFERENCES

[1] ET. AL, M. F. Cardiovascular magnetic resonance in myocarditis: A jacc white paper. *Journal of the American College of Cardiology 53*, 17 (2009), 1475–1487.

[2] P, C., AND D, J.-N. A review of segmentation methods in short axis cardiac mr images. *Medical image analysis 15*, 2 (2011), 169–184.

[3] PETITJEAN, C., ZULUAGA, M. A., BAI, W., DACHER, J.-N., GROSGEORGE, D., CAUDRON, J., RUAN, S., AYED, I. B., CARDOSO, M. J., CHEN, H.-C., JIMENEZ-CARRETERO, D., LEDESMA-CARBAYO, M. J., DAVATZIKOS, C., DOSHI, J., ERUS, G., MAIER, O. M., NAMBAKHSH, C. M., OU, Y., OURSELIN, S., PENG, C.-W., PETERS, N. S., PETERS, T. M., RAJCHL, M., RUECKERT, D., SANTOS, A., SHI, W., WANG, C.-W., WANG, H., AND YUAN, J. Right ventricle segmentation from cardiac mri: A collation study. *Medical Image Analysis 19*, 1 (2015), 187 – 202.

[4] ET. AL., M. F. Characterization of motion cardiac patterns in magnetic resonance cine. In *Image Information Processing (ICIIP),* (2011), IEEE, pp. 1–5.

[5] ET. AL., C. F. The cardiac atlas project—an imaging database for computational modeling and statistical atlases of the heart. *Bioinformatics 27*, 16 (2011), 2288–2295.

[6] T, P. V. A fully convolutional neural network for cardiac segmentation in short-axis mri. *arXiv preprint arXiv:1604.00494* (2016).

[7] HAJIAGHAYI, M., GROVES, E. M., JAFARKHANI, H., AND KHERADVAR, A. A 3-d active contour method for automated segmentation of the left ventricle from magnetic resonance images. *IEEE Transactions on Biomedical Engineering 64*, 1 (Jan 2017), 134–144.

[8] Dakua, S. P. Towards left ventricle segmentation from magnetic resonance images. *IEEE Sensors Journal 17*, 18 (Sept 2017), 5971–5981.

[9] Wang, Z. Z. Segmentation of the left ventricle in short-axis sequences by combining deformation flow and optical flow. *IET Image Processing 11*, 4 (2017), 237–244.

[10] Labrador, A. M. A., Martínez, F., and Castro, E. R. *A Novel Right Ventricle Segmentation Approach from Local Spatio-temporal MRI Information*. Springer Berlin Heidelberg, Berlin, Heidelberg, 2013, pp. 206–213.

[11] Bernard, O., Lalande, A., Zotti, C., Cervenansky, F., Yang, X., Heng, P. A., Cetin, I., Lekadir, K., Camara, O., Ballester, M. A. G., Sanroma, G., Napel, S., Petersen, S., Tziritas, G., Grinias, E., Khened, M., Kollerathu, V. A., Krishnamurthi, G., Rohé, M. M., Pennec, X., Sermesant, M., Isensee, F., Jäger, P., Maier-Hein, K. H., Baumgartner, C. F., Koch, L. M., Wolterink, J. M., Išgum, I., Jang, Y., Hong, Y., Patravali, J., Jain, S., Humbert, O., and Jodoin, P. M. Deep learning techniques for automatic mri cardiac multi-structures segmentation and diagnosis: Is the problem solved? *IEEE Transactions on Medical Imaging* (2018), 1–1.

[12] Petitjean, C., and Dacher, J.-N. A review of segmentation methods in short axis cardiac mr images. *Medical Image Analysis 15*, 2 (2017/11/10 XXXX), 169–184.

[13] El-Rewaidy, H., Ibrahim, E. S., and Fahmy, A. S. Segmentation of the right ventricle in mri images using a dual active shape model. *IET Image Processing 10*, 10 (2016), 717–723.

[14] Sedai, S., Garnavi, R., Roy, P., and Liang, X. Multi-atlas label fusion using hybrid of discriminative and generative classifiers for segmentation of cardiac mr images. In *2015 37th Annual International Conference of the IEEE Engineering in Medicine and Biology Society (EMBC)* (Aug 2015), pp. 2977–2980.

[15] Xie, L., Sedai, S., Liang, X., Compas, C. B., Wang, H., Yushkevich, P. A., and Syeda-Mahmood, T. Multi-atlas label fusion with augmented atlases for fast and accurate segmentation of cardiac mr images. In *2015 IEEE 12th International Symposium on Biomedical Imaging (ISBI)* (April 2015), pp. 376–379.

[16] ET. AL, A. M. A combined deep-learning and deformable-model approach to fully automatic segmentation of the left ventricle in cardiac mri. *Medical image analysis 30* (2016), 108–119.

[17] KHEMPHILA, A., AND BOONJING, V. Heart disease classification using neural network and feature selection. In *Systems Engineering (ICSEng)* (2011), IEEE, pp. 406–409.

[18] MANZANERA, A. Dense hough transforms on gray level images using multi-scale derivatives. In *SIXIEME WORKSHOP AMINA 2012 Applications Médicales de l´Informatique : Nouvelles Approches* (Dec 2012), hal-01119654.

[19] DUFFNER, S., AND GARCIA, C. Pixeltrack: a fast adaptive algorithm for tracking non-rigid objects. In *Proceedings of the International Conference on Computer Vision (ICCV)* (Sidney, AUS, Dec. 2013).

[20] LUO, G., AN, R., WANG, K., DONG, S., AND ZHANG, H. A deep learning network for right ventricle segmentation in short-axis mri. In *2016 Computing in Cardiology Conference (CinC)* (Sept 2016), pp. 485–488.

[21] EL-REWAIDY, H., IBRAHIM, E. S., AND FAHMY, A. S. Segmentation of the right ventricle in mri images using a dual active shape model. *IET Image Processing 10*, 10 (2016), 717–723.

[22] EL-REWAIDY, H., AND FAHMY, A. S. Segmentation of the right ventricle in mr images using dual active shape model in the bookstein coordinates. In *2015 IEEE 12th International Symposium on Biomedical Imaging (ISBI)* (April 2015), pp. 1320–1323.

[23] MAIER, O. M. O., JIMÉNEZ, D., SANTOS, A., AND LEDESMA-CARBAYO, M. J. Segmentation of rv in 4d cardiac mr volumes using region-merging graph cuts. In *2012 Computing in Cardiology* (Sept 2012), pp. 697–700.

[24] ZULUAGA, M. A., CARDOSO, M. J., MODAT, M., AND OURSELIN, S. Multi-atlas propagation whole heart segmentation from mri and cta using a local normalised correlation coefficient criterion. In *Functional Imaging and Modeling of the Heart* (Berlin, Heidelberg, 2013), S. Ourselin, D. Rueckert, and N. Smith, Eds., Springer Berlin Heidelberg, pp. 174–181.

[25] Bai, W., Shi, W., Wang, H., Peters, N. S., and Rueckert, D. Multi-atlas based segmentation with local label fusion for right ventricle mr images.

[26] Grosgeorge, D., Petitjean, C., Dacher, J.-N., and Ruan, S. Graph cut segmentation with a statistical shape model in cardiac mri. *Computer Vision and Image Understanding 117*, 9 (2013), 1027 – 1035.

[27] Sarmiento, E., Pico, J., and Martinez, F. Cardiac disease prediction from spatio-temporal motion patterns in cine-mri. In *2018 IEEE 15th International Symposium on Biomedical Imaging (ISBI 2018)* (April 2018), pp. 1305–1308.

[28] Brox, T., and Malik, J. Large displacement optical flow: descriptor matching in variational motion estimation. *IEEE PAMI 33*, 3 (2011), 500–513.

[29] Chang, C.-C., and Lin, C.-J. Libsvm: a library for support vector machines. *ACM transactions on intelligent systems and technology (TIST) 2*, 3 (2011), 27.

[30] et. al., R. P. Evaluation framework for algorithms segmenting short axis cardiac mri. *The MIDAS Challenge 49* (2009).

BIBLIOGRAPHY

BAI, W., *et al.* (2012). Multi-atlas based segmentation with local label fusion for right ventricle mr images.

BERNARD, O., *et al.* (2018). Deep learning techniques for automatic mri cardiac multi-structures segmentation and diagnosis:Is the problem solved?, IEEE Transactions on Medical Imaging, pages 1–1.

BROX, T. and MALIK, J. (2011). Large displacement optical flow: descriptor matching in variational motion estimation.IEEE PAMI, 33(3):500–513.

CHANG, C.-C. and LIN, C.-J. (2011). Libsvm: a library for support vector machines.ACM transactions on intelligent systems and technology (TIST), 2(3):27.

DAKUA, S. P. (2017). Towards left ventricle segmentation from magnetic resonance images.IEEE Sensors Journal, 17(18):5971–5981.

DUFFNER, S. and GARCIA, C. (2013). Pixeltrack: a fast adaptive algorithm for tracking non-rigid objects. In Proceedings of the International Conference on Computer Vision(ICCV), Sidney, AUS.

EL-REWAIDY, H. and FAHMY, A. S. (2015). Segmentation of the right ventricle in mr images using dual active shape model in the bookstein coordinates. In2015 IEEE12th International Symposium on Biomedical Imaging (ISBI), pages 1320–1323.

EL-REWAIDY, H., IBRAHIM, E. S., and FAHMY, A. S. (2016a). Segmentation of the right ventricle in mri images using a dual active shape model.IET Image Processing,10(10):717–723.

et. al, A. M. (2016). A combined deep-learning and deformable-model approach to fully automatic segmentation of the left ventricle in cardiac mri.Medical image analysis, 30:108–119.

et. al., C. F. (2011a). The cardiac atlas project—an imaging database for computational modeling and statistical atlases of the heart.Bioinformatics, 27(16):2288–2295.

et. al, M. F. (2009). Cardiovascular magnetic resonance in myocarditis: A jaccwhite paper.Journal of the American College of Cardiology, 53(17):1475–1487.

et. al., M. F. (2011b). Characterization of motion cardiac patterns in magnetic resonance cine. In Image Information Processing (ICIIP)„ pages 1–5. IEEE.

et. al., R. P. (2009). Evaluation framework for algorithms segmenting short axis cardiac mri.The MIDAS Challenge, 49.

GROSGEORGE, D., *et al.* (2013). Graph cut segmentation with a statistical shape model in cardiac mri.Computer Vision and Image Understanding, 117(9):1027 – 1035.

HAJIAGHAYI, M., GROVES, E. M., JAFARKHANI, H., and KHERADVAR, A. (2017). A 3-d active contour method for automated segmentation of the left ventricle from magnetic resonance images.IEEE Transactions on Biomedical Engineering, 64(1):134–144.

KHEMPHILA, A. and BOONJING, V. (2011). Heart disease classification using neural network and feature selection. In Systems Engineering (ICSEng), pages 406–409.IEEE.

LABRADOR, A. M. A., MARTINEZ, F., and CASTRO, E. R. (2013).A Novel Right Ventricle Segmentation Approach from Local Spatio-temporal MRI Information, pages206–213. Springer Berlin Heidelberg, Berlin, Heidelberg.

LUO, G., An, R., WANG, K., DONG, S., and ZHANG, H. (2016). A deep learning network for right ventricle segmentation in short-axis mri. In2016 Computing in Cardiology Conference (CinC), pages 485–488.

MAIER, O. M. O., JIMENEZ, D., SANTOS, A., and LEDESMA-CARBAYO, M. J. (2012).Segmentation of rv in 4d cardiac mr volumes using region-merging graph cuts. In2012 Computing in Cardiology, pages 697–700.

MANZANERA, A. (Dec 2012). Dense hough transforms on gray level images using multi-scale derivatives. In SIXIEME WORKSHOP AMINA 2012 Applications Médicales de l Informatique : Nouvelles Approches. hal-01119654.

P, C. and D, J.-N. (2011). A review of segmentation methods in short axis cardiac mr images.Medical image analysis, 15(2):169–184.

PETITJEAN, C. and DACHER, J.-N.. A review of segmentation methods in short axis cardiac mr images.Medical Image Analysis, 15(2):169–184.

Petitjean, C., *et al.* (2015).Right ventricle segmentation from cardiac mri: A collation study.Medical Image Analysis, 19(1):187 – 202.

SARMIENTO, E., PICO, J., and MARTINEZ, F. (2018). Cardiac disease prediction from spatio-temporal motion patterns in cine-mri. In2018 IEEE 15th International Symposium on Biomedical Imaging (ISBI 2018), pages 1305–1308.

SEDAI, S., GARNAVI, R., ROY, P., and LIANG, X. (2015). Multi-atlas label fusion using hybrid of discriminative and generative classifiers for segmentation of cardiac mr images. In2015 37th Annual International Conference of the IEEE Engineering in Medicine and Biology Society (EMBC), pages 2977–2980.

T, P. V. (2016). A fully convolutional neural network for cardiac segmentation in short-axis mri.arXiv preprint arXiv:1604.00494.

WANG, Z. Z. (2017). Segmentation of the left ventricle in short-axis sequences by combining deformation flow and optical flow.IET Image Processing, 11(4):237–244.

XIE, L., *et al.* (2015). Multi-atlas label fusion with augmented atlases for fast and accurate segmentation of cardiac mr images. In2015 IEEE 12th International Symposium on Biomedical Imaging (ISBI), pages 376–379.

ZULUAGA, M. A.,*et al.*, editors,Functional Imaging and Modeling of the Heart, pages 174–181, Berlin, Heidelberg.Springer Berlin Heidelberg.

Appendices

APPENDIX A

Second scenario: Cardiac Disease Classification

A.1 Second scenario: Cardiac Disease Classification

This scenario was part of a collaborative work between members of the Biomedical Engineering research group - GIIB at the Universidad Industrial de Santander. This work was published in the IEEE International Symposium on Biomedical Imaging (ISBI 2018)[27]. In addition, it was presented in poster modality by me at Washington, D.C. on April 6th. My main contribution was the automatic detection and tracking of right and left ventricles in MRI sequences by using Dense Hough Transform. Next, the method is presented.

Cardiac Hough representation was successfully implemented to detect heart chambers along the cardiac cycle regionally. In this disease classification scenario, regions of interest (RoIs) were firstly automatically detected from a fast dense Hough template representation. Then, over the selected RoIs was computed a dense optical flow with the ability to characterize large local displacements. Spatial regional segmentation of RoIs was carried out by using a circular template, where dense orientation flow histograms characterize each subregion. The set of subregions motion histograms form the motion descriptor that is mapped to a previously trained support vector machine (SVM) to predict cardiac pathologies.

A.1.1 Motion heart characterization Cardiac motion quantification is the main issue for analysis and characterization of abnormal heart patterns. Never-

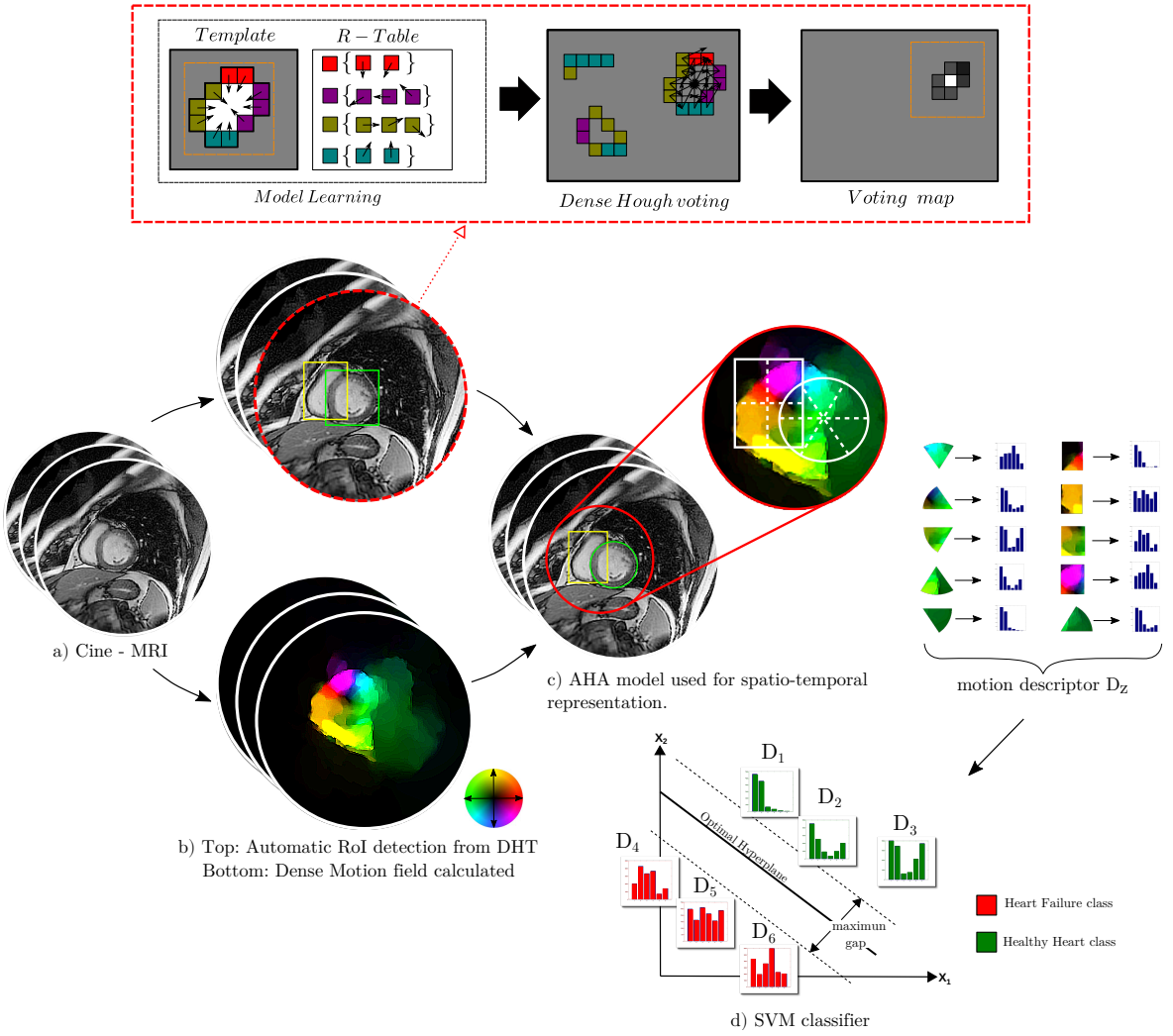

Figure 14. (a) cine- MRI from Dataset. (b) First, an automatic heart and ventricles detection is carried out by using Dense Hough transform (DHT). (b) In parallel, a dense optical flow is computed over the projected cine-MRI. In (c) is computed motion histograms by each sub-region of RoI. Finally, in (d) the set of motion histograms are mapped to a SVM.

theless, such analysis is challenging because the nonlinear heart displacements and the continuous deformation of heart chambers along the cardiac cycle. In this approach, a dense optical flow that considers large local displacements [28] was implemented to characterize Hough detected regions. This motion strategy based on a variational flow approach is based on classical color $E_{color}(w)$ and gradient $E_{gradient}(w)$ constraints, that assume that appearance and local geometry is close similar among consecutive frames. Also, the strategy introduces a flow dispersion constraint $E_{smooth}(w)$ that as-

sume smooth changes of the field along the sequence. Finally a non-local regional $E_{desc}(w_1)$ constraint is achieved by computing a local matching of SIFT points in consecutive frames and then comparing the computed flow in such non-local regions. The sum of whole constraints is considered to find an optical field.

A.1.2 Spatio-temporal motion AHA-like coding

Then, a set of optical flow histograms were computed over specific segments in detected RoIs $\zeta_{\mathbf{x}}$. These histograms quantify a set of occurrence orientation, weighted by the norm of each velocity vector. The representation of each histogram is given by $h(k) = \sum_{\mathbf{x}\in I} S_k(\mathbf{x})||\nabla w(\mathbf{x})||$, where $||\nabla w(\mathbf{x})||$ is the magnitude of each vector flow.

Such orientation flow histograms are computed regionally according to the model suggested for American Heart Association (AHA) that group segments of the heart according to motion information. This AHA model is widely used by physicians to report abnormal regions in heart and to diagnose specific pathologies according to the regional exam.

Once the spatio-temporal histograms are computed for each sub-region and the different RoIs, they are group up in a single motion descriptor that summarizes the performance of a particular cine-MRI sample. The recognition of each potential heart condition in a cine-MRI was carried out by a Support Vector Machine (SVM) classifier [29].

A.2 Results

The evaluation of the proposed Cardiac Disease Classification was performed over the public Cardiac cine-MRI dataset **Sunnybrook Cardiac Data (SCD)** [30]. The 45 recorded patients were diagnosed with four cardiac pathologies like hypertrophy (HYP), heart failure with infarction (HF-I), heart failure without infarction (HF) and healthy (N). The data is split into 15 women and 32 men cases, respectively. The RoIs corresponding to left ventricle was split into 6 subregions from a circular template. The Right ventricle RoIs were split in four. Each of the subregions was characterized by using flow orientation histograms of 6. A leave-one-out cross-validation was performed into a binary classification scheme.

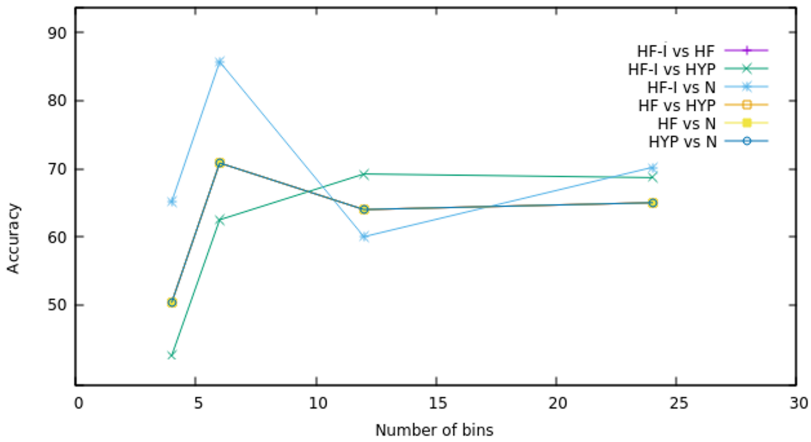

Figure 15. Accuracy of the proposed approach according to the number of bins.

Table 4 summarizes the accuracy obtained by the proposed approach, evaluating pairs of heart disease classes. In average was achieved 70.7% of accuracy, showing a proper performance prediction for the trained pathologies with a descriptor of 1140 scalar values. The proposed approach was evaluated with a binary classification in order to obtain fast predictions, an essential requirement for real clinical protocols.

Table 1. An automatic classification of heart pathologies between a pair of classes.

Heart pathologies	Avg Acc (%)
HF-I vs HF	70.83
HF-I vs HYP	62.5
HF-I vs N	**85.71**
HF vs HYP	62.5
HF vs N	80.95
HYP vs N	61.69

Finally, in Figure 10 is illustrated the performance of the proposed approach by using a different number of flow orientation histograms to represent each subregion. This number of bins define the dimension of the descriptor, and it is directly related to the computational complexity to carried out the prediction. A total of 6 bins were sufficient to represent each subregion of the RoIs, and 60 by a slice, with a total descriptor dimension of 1140 for each cine-MRI.